

# SCIENTIFIC REPORTS



OPEN

## Multicolor Colormetric Biosensor for the Determination of Glucose based on the Etching of Gold Nanorods

Received: 22 September 2016

Accepted: 02 November 2016

Published: 25 November 2016

Yue Lin<sup>1</sup>, Mengmeng Zhao<sup>1</sup>, Yajuan Guo<sup>1</sup>, Xiaoming Ma<sup>1</sup>, Fang Luo<sup>2</sup>, Longhua Guo<sup>1</sup>, Bin Qiu<sup>1</sup>, Guonan Chen<sup>1</sup> & Zhenyu Lin<sup>1</sup>

In this work, 3,3',5,5'-tetramethylbenzidine(II) (TMB<sup>2+</sup>), derived from H<sub>2</sub>O<sub>2</sub>-horseradish peroxidase (HRP)-3,3',5,5'-tetramethylbenzidine (H<sub>2</sub>O<sub>2</sub>-HRP-TMB) reaction system, was used to etch AuNRs to generate different colors of solution. Many enzyme reactions are involved in the production of H<sub>2</sub>O<sub>2</sub> (e.g., glucose can react with the dissolved oxygen in the presence of glucose oxidase (GOx) to produce H<sub>2</sub>O<sub>2</sub>). Given this information, a simple visual biosensor was developed in this study, with glucose as the example target. The detection range of the proposed system varied with the experimental conditions, such as the concentration of GOx and HRP, and enzymatic reaction time. Under the optimized conditions, the longitudinal shift of localized surface plasmon resonances (LSPR) had a linear correlation with the glucose concentration in the range of 0.1–1.0 mM. Meanwhile, the solution displayed a specific color in response to the glucose concentration, thus enabling the visual quantitative detection of glucose at a glance. Compared with the traditional monochromic colorimetry, this multicolor glucose sensor generates various vivid colors, which can be easily distinguished by naked eyes without any sophisticated instrument. Notably, the proposed method has been successfully applied to detect glucose in serum samples with satisfied results.

The solution of noble metals is normally colored in view of their fascinating size-dependent properties. The color is mainly controlled by their shape, size, and composition, resulting in great wide application prospect in electronics, catalysis, optics, and biosensing<sup>1,2</sup>. Among these noble metals, gold nanoparticles (AuNPs) exhibit strong localized surface plasmon resonances (LSPRs) within the visible or near-IR, making them broadly used in colorimetric chernosensor<sup>3,4</sup>. Gold nanorods (AuNRs) possess a typical plasmonic one-dimensional nanostructure with two separate surface plasmon resonances (SPR) bands corresponding to transverse and longitudinal peak, respectively, the longitudinal peak is sensitive to their aspect ratio. Different optical signals can be acquired in a wide range of wavelength by simply adjusting the aspect ratio<sup>5</sup>. Based on these characters, AuNRs have gained increasing attention and how to change their aspect ratio becomes a problem worthy of exploring in various application fields. To date, many post-synthetic morphological methods have been proposed for modifying AuNRs such as transverse overgrowth<sup>6</sup>, shorting<sup>7</sup>, and lateral etching<sup>8</sup>. A promising detection method based on the etching of AuNRs by H<sub>2</sub>O<sub>2</sub> has been recently reported<sup>9,10</sup>. Vivid color changes were presented. However, it still faced with some disadvantages. For example, several hours are required to proceed the oxidation of AuNRs with high concentration of H<sub>2</sub>O<sub>2</sub> and specific pH, making it possess biological destructiveness and hence difficult to be applied in biological detection systems.

To significantly improve the performance of the sensing systems, aplenty of enzymes and metal ions have been employed to shorten the detection time due to their catalytic property. Numerous plasmonic sensors and other similar ones have been developed and applied to detect diverse targets other than H<sub>2</sub>O<sub>2</sub>, such as Cu<sup>2+</sup>, Fe<sup>3+</sup>, CN<sup>-</sup>, NO<sub>2</sub><sup>-</sup>, Cl<sup>-</sup> and Hg<sup>+</sup> ions<sup>11–17</sup>. Methods for Cu<sup>2+</sup> detection was proposed via the etching of AuNRs by H<sub>2</sub>O<sub>2</sub>

<sup>1</sup>MOE Key Laboratory of Analysis and Detection for Food Safety, Fujian Provincial Key Laboratory of Analysis and Detection Technology for Food Safety, Institute of Nanomedicine and Nanobiosensing, College of Chemistry, Fuzhou University, Fuzhou, Fujian 350116, China. <sup>2</sup>College of Biological Science and Technology, Fuzhou University, Fuzhou, Fujian 350116, China. Correspondence and requests for materials should be addressed to L.G. (email: guolh@fzu.edu.cn) or Z.L. (email: zylin@fzu.edu.cn)

because  $\text{Cu}^{2+}$  can catalyze  $\text{H}_2\text{O}_2$ -AuNRs etching system<sup>18,19</sup>. A promising strategy was reported to detect  $\text{Fe}^{3+}$  through selective etching of Au NRs at room temperature<sup>13</sup>. A method was developed for blood glucose detection based on enzymatic etching of AuNRs by horseradish peroxidase (HRP)<sup>20</sup>. High concentration of HRP, however, is needed in this system, which extremely limits the reaction conditions. Based on the similar principle, a plasmonic monitor was proposed for blood glucose<sup>21</sup>. Nevertheless all these chromogenic processes in sensors cannot be terminated or kept stable at a fixed time range (for easily discrimination). Furthermore, the color change cannot be easily distinguished by naked eyes.

HRP- $\text{H}_2\text{O}_2$ -3,3',5,5'-tetramethylbenzidine (TMB) system has been used to quantify  $\text{H}_2\text{O}_2$  frequently and this principle has been coupled with enzymatic reaction (which can produce  $\text{H}_2\text{O}_2$ ) to detect diverse targets with high selectivity. In this study, the product of  $\text{H}_2\text{O}_2$ -HRP-TMB-HCl catalyzed oxidation system, 3,3',5,5'-tetramethylbenzidine(II) ( $\text{TMB}^{2+}$ ), quantitatively etched AuNRs to produce different vivid color solutions<sup>22</sup>, meanwhile, the addition of HCl can inactivate effectively HRP to keep the oxidizing reaction stable. Because the  $\text{TMB}^{2+}$  has direct relationship with  $\text{H}_2\text{O}_2$  and  $\text{H}_2\text{O}_2$  can be generated from glucose-GOx reaction system, glucose was chosen as the example. A novel multicolor glucose sensor utilizing  $\text{TMB}^{2+}$ -AuNRs as chromogenic substrate is presented to realize the visual quantitative detection of glucose by naked eyes. The multicolor glucose sensor displays advantages of speediness, simplicity, visualization as well as low cost, enabling this system to be a potentially powerful tool for the investigation of blood glucose in clinical examination, especially for some poor areas lacking expert medical facilities.

## Methods

**Materials and Instruments.** TMB, HRP,  $\text{HAuCl}_4$  and glucose were acquired from Aladdin (Shanghai, China), while the cetyltrimethyl ammonium bromide (CTAB) was obtained from J&K Chemical Technology (Beijing, China) and the ascorbic acid (AA) was supplied by Fu Chen Chemistry (Tianjin, China). Amino acids,  $\text{NaBH}_4$ ,  $\text{AgNO}_3$ , and  $\text{H}_2\text{O}_2$  were purchased from Sinopharm (Shanghai, China). GOx was purchased from Sangon (Shanghai, China). All used water was ultrapure water ( $18.2 > \text{M}\Omega \cdot \text{cm}$ ) from Direct-Q3 UV system (Millipore). Ultraviolet-visible (UV-Vis) absorption spectra were recorded by Multiskan spectrum microplate spectrophotometer (Thermo, USA) and UV-Vis absorption spectroscopy (1102UV-Vis spectrophotometer, Techcomp, China).

**Preparation of Gold Nanorods.** According to the previously reported literature<sup>7</sup>, AuNRs were synthesized with slight modification. Briefly, 0.25 mL of  $\text{HAuCl}_4$  (0.01 M) mixed with 5 mL of CTAB (0.2 M) in a 20 mL glass bottle under water bath (30 °C). 0.6 mL of  $\text{NaBH}_4$  (0.01 M) freshly prepared by ice distilled water was rapidly added to the glass bottle, followed by vigorous inversion (1200 r/min) for 5 min. The color of the liquid changing from dark yellow to brown indicated the formation of seed solution. Keep it stationary at room temperature for at least 10 min. Subsequently, 100 mL of CTAB (0.2 M) was added to 1.25 mL of  $\text{AgNO}_3$  (0.01 M) in 250 mL florence flask with vigorous stirring (700 r/min) for 2 min, and then 10 mL of  $\text{HAuCl}_4$  (0.01 M) was introduced to the mixture. The final mixture was continuously stirred for 2 min. 11 mL of ascorbic acid (0.01 M, AA) was slowly dripped into the resulting mixture until the color turned from pale yellow to colourless. Finally, 0.4 mL of seed solution was quickly added to resultant mixture with sufficient oscillation for 20 sec. Keep it at 30 °C in a water bath for at least 3 h to ensure full growth of AuNRs. The CTAB on the surface of AuNRs was removed by centrifugation and the resulting concentrated AuNRs solution was kept in a 20 mL brown glass bottle to extend the shelf-life.

**Visual Detection of Glucose.** 20 mL of CTAB solution (0.2 M) initially mixed with concentrated AuNRs solution at a volume ratio of 4:1. Different concentrations of glucose (50  $\mu\text{L}$ ) were added to 96-well plates at room temperature, and then 400  $\mu\text{L}$  of GOx (0.1 mg/mL), 400  $\mu\text{L}$  of HRP (4  $\mu\text{g}/\text{mL}$ ) and 1 mL of TMB liquid substrate were added to the 4 mL centrifuge tube with sufficient mixing. Subsequently, 90  $\mu\text{L}$  of obtained solution was added to glucose in the 96-well plates, the light blue slowly appeared and deepened over time. After enzymatic reaction (20 min), 10  $\mu\text{L}$  of HCl (5 M) was introduced to the mixture to end the reaction. The color quickly turned to yellow, suggesting  $\text{TMB}^{2+}$  was produced<sup>23</sup>. 100  $\mu\text{L}$  of AuNRs-CTAB mixture was eventually added to the 96-well plates. After sufficient reaction (within 60 s), the absorption spectra ranging from 300 to 900 nm were recorded using the Multiskan spectrum microplate spectrophotometer.

**Detection of Glucose in Serum Samples.** Different serum samples were diluted with PBS (0.01 M, pH7.4) at a volume ratio of 1:9. Then 50  $\mu\text{L}$  of diluent solution was added to the 96-well plates. In parallel, 50  $\mu\text{L}$  of distilled water was added to the other well and the next procedure was the same as the abovementioned process for glucose sensing.

## Results and Discussion

**Principle of the Proposed Multicolor Glucose Sensor.** Figure 1 schematically depicts the principle of the proposed multicolor sensor. With the assistant of GOx, glucose reacts with the dissolved oxygen to produce  $\text{H}_2\text{O}_2$ .  $\text{TMB}^0$  is then oxidized to blue  $\text{TMB}^+$  by  $\text{H}_2\text{O}_2$  in the presence of HRP. After the addition of HCl, HRP is inactivated and the yellow  $\text{TMB}^{2+}$  is produced. However, the  $\text{TMB}^{2+}$  just presents various shades of yellow, which is difficult for discrimination of human eyes. Then the mixture solution of AuNRs and CTAB is added to the  $\text{TMB}^{2+}$  solution with sufficient mixing. AuNRs can react with  $\text{TMB}^{2+}$  to produce  $\text{TMB}^0$ , and meanwhile Au was oxidized into Au(I). This oxidation process selectively takes place at the ends of AuNRs<sup>7</sup>. Thus, the visual glucose detection can be achieved based on the etching of AuNRs. Different levels of etching and various colors of the solution respond directly to different concentrations of glucose. The final obtained solution is rich-colored, several colors such as pink, purple, blue, green and grey at different glucose concentrations can be distinguished at a glance. When the AuNRs are completely oxidized, only  $\text{TMB}^{2+}$  exists and the color changes to yellow. Based on these phenomena, a pretty simple multicolor biosensor was developed for the determination of glucose.

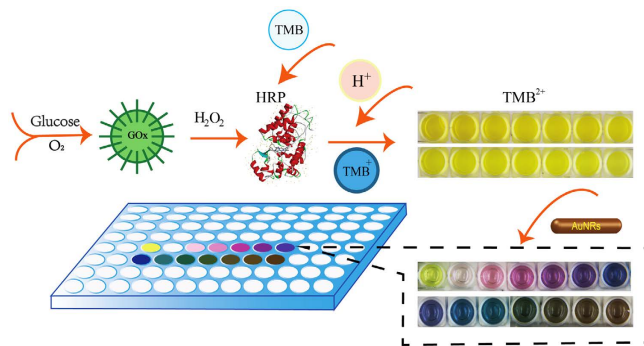


**Figure 1.** Presentation of multicolor glucose sensor by the oxidation of Au NRs.

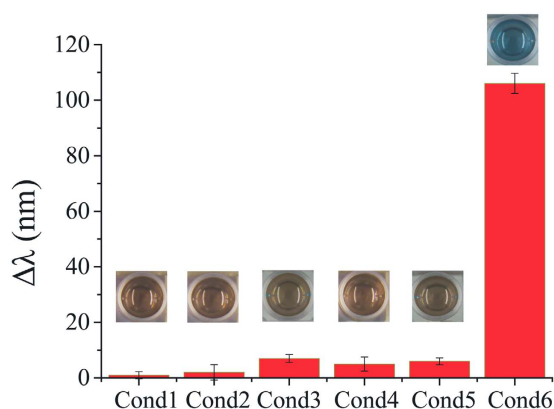


**Figure 2.** The LSPR shift of Au NRs under different conditions. (Cond 1: Glucose + GOx + HRP + AuNRs; Cond 2: Glucose + HRP + TMB + HCl + AuNRs; Cond 3: GOx + HRP + TMB + HCl + AuNRs; Cond 4: Glucose + GOx + TMB + HCl + AuNRs; Cond 5: Glucose + GOx + HRP + HCl + AuNRs; Cond 6: Glucose + GOx + HRP + TMB + HCl + AuNRs). The insets show the solution color of the corresponding conditions.

Control experiments were carried out to demonstrate the feasibility of the proposed system. Figure 2 shows the performance of the system under different conditions. Under the several conditions without the addition of HCl and TMB, GOx, glucose, HRP, or TMB, respectively, no color change was observed, indicating the unsuccessful etching of AuNRs. Whereas the color of the solution changed quickly when all reagents were simultaneously added, indicating the successful etching of AuNRs. These results confirm the feasibility of principle. Figure 3 displays the TEM image and the corresponding SPR absorption spectrum of AuNRs without addition of  $\text{TMB}^{2+}$ . While Fig. 3B,C and D show the TEM images and the SPR absorption spectra of AuNRs with addition of different amounts of glucose and the rest of reagent (used to produce different quantity of  $\text{TMB}^{2+}$ ). With the increase of glucose concentration, the length of AuNRs decreased gradually, at the same time, the longitudinal LSPR shifted blue and the solution displayed different colors. Notably, these results also verify the feasibility of principle.

**Optimization of the Reaction Conditions.** The concentration of GOx and HRP, and enzymatic reaction time have a great influence on the performance of the proposed biosensor because they affect the amount of  $\text{H}_2\text{O}_2$  produced. Given that the normal blood glucose in the human serum ranges from 3.9 to 7.8 mM, to reduce the potential interference, the sample was diluted for 10 times before examination. To fit the real glucose level in human serum, the sensing range was controlled from 0.1 to 1.0 mM. Excessive amount of GOx (0.01 mg/mL) was added and the enzymatic reaction was fixed at 20 min for easy detection.

The concentration of HRP was optimized firstly. As shown in Fig. 4A, the longitudinal peak shift of AuNRs increased with the augment of HRP concentration at different levels of glucose, and then reached a plateau when higher than 4  $\mu\text{g/mL}$ . So 4  $\mu\text{g/mL}$  of HRP was chosen as the optimal condition. CTAB also plays an important role in the proposed multicolor sensor system. In the absence of CTAB, the standard electrode potential of  $\text{AuBr}^{2-}/\text{Au}$  (0.93 V vs NHE) ( $E^\ominus$ ) was lower than  $\text{TMB}^{2+}/\text{TMB}$  (0.741 V vs NHE), preventing the oxidation of AuNRs by  $\text{TMB}^{2+}$ . Upon the addition of CTAB, the reduction potential of  $\text{AuBr}^{2-}/\text{Au}$  reduced via forming  $\text{AuBr}^{2-} - (\text{CTA})^{2+}/\text{Au}$  ( $E^\ominus < 0.2 \text{ V vs NHE}$ ), facilitating the oxidation of AuNRs<sup>24</sup>. The concentration of CTAB was optimized as well, and the result showed that as CTAB concentration rose, the longitudinal peak shift of AuNRs first increased rapidly and then kept stable when its concentration exceeded 0.12 M (Fig. 4B). So 0.12 M was chosen as the optimal concentration of CTAB. HCl in this detection is used to inactive HRP to stop the reaction, so it

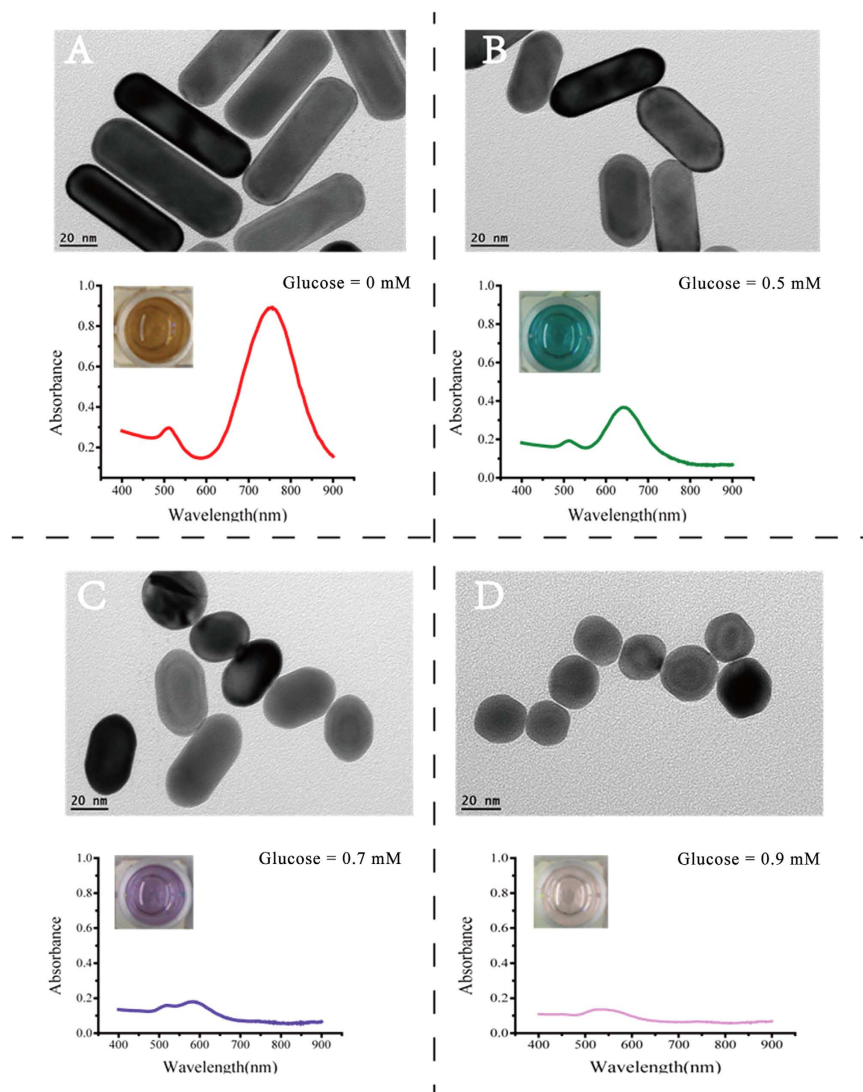


**Figure 3.** The UV-Vis absorption spectra and TEM images of AuNRs before and after etching with different concentrations of  $\text{TMB}^{2+}$ . The insets show the colors of the corresponding solutions.

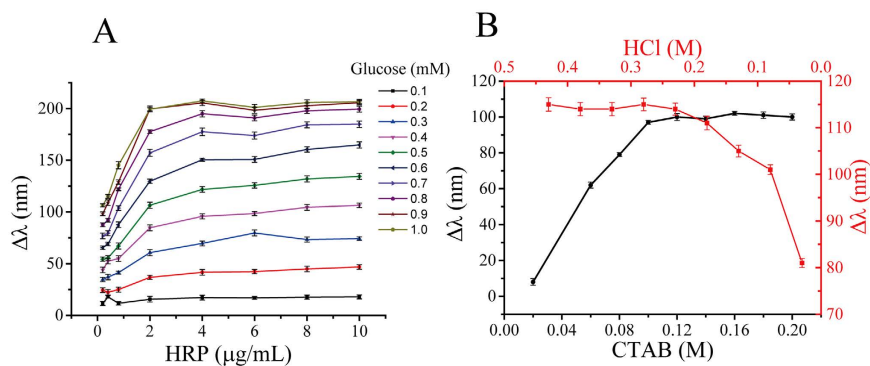


**Figure 4.** (A) The LSPR shift of AuNRs with various concentrations of HRP (initial concentrations: 0.4, 0.6, 0.8, 2.0, 4.0, 6.0, 8.0, 10.0  $\mu\text{g/mL}$ , respectively); (B) The LSPR shift of AuNRs with various concentrations of CTAB (initial concentrations: 0.03, 0.06, 0.10, 0.12, 0.13, 0.14, 0.16, 0.18, 0.20 M, respectively) and HCl (initial concentrations: 0.03, 0.08, 0.13, 0.18, 0.23, 0.28, 0.33, 0.38, 0.43 M, respectively).

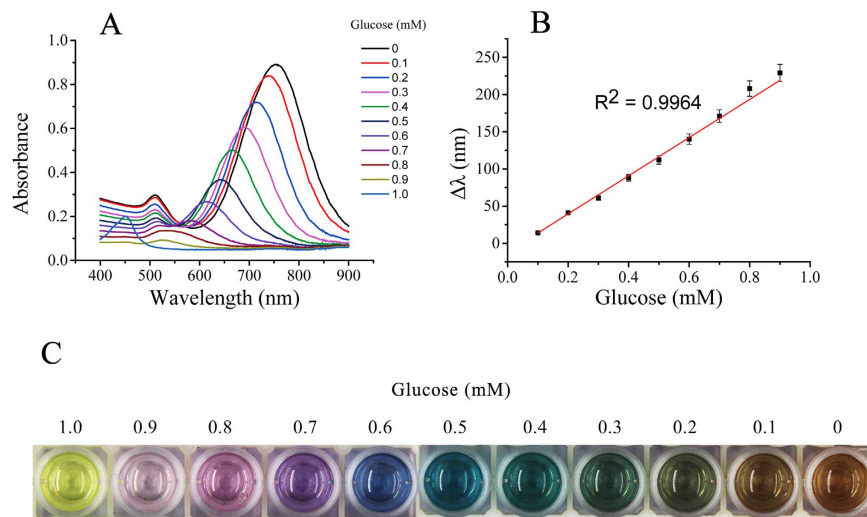


**Figure 5.** (A) The UV-Vis spectra change of AuNRs in the oxidation etching process with different concentrations of glucose; (B) The LSPR shift of AuNRs as a function of glucose concentration; (C) Color change of the plasmonic sensor with the decrease of glucose concentrations.

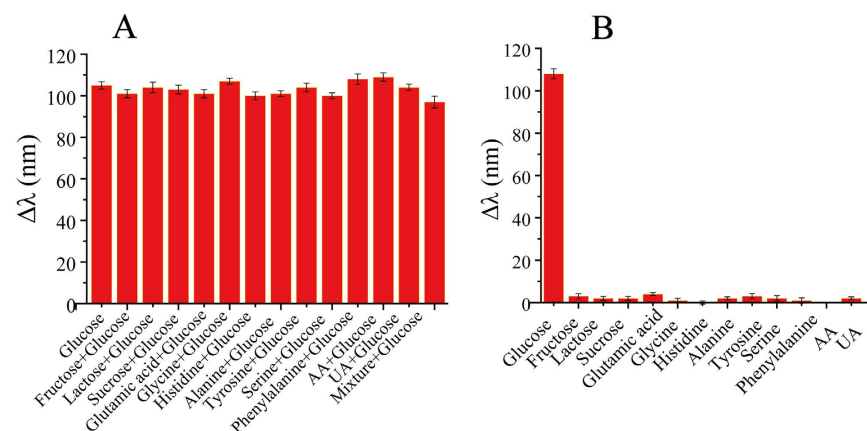


**Figure 6.** Selectivity tests of the multicolor glucose sensor to normal interference in traditional glucose assay.  $\Delta\lambda$ : the LSPR shift of the AuNRs in response to (A) 0.5 mM glucose, 1 mM Fructose, 1 mM Lactose, 1 mM sucrose, 30 mM Glutamic acid, 10 mM Glycine, 10 mM Histidine, 30 mM Alanine, 30 mM Tyrosine, 30 mM Serine, 6 mM Phenylalanine, 1 mM AA and 1 mM UA and (B) the mixture of 0.5 mM glucose and 1 mM Fructose, 1 mM Lactose, 1 mM sucrose, 30 mM Glutamic acid, 10 mM Glycine, 10 mM Histidine, 30 mM Alanine, 30 mM Tyrosine, 30 mM Serine, 6 mM Phenylalanine, 1 mM AA and 1 mM UA.

is necessary to explore how the presence of HCl affects the detection results. As shown in Fig. 4B, the longitudinal peak shift of AuNRs was increased with the addition of HCl and then reaches a plateau when the concentration of HCl was over 0.23 M. So, 0.23 M was chosen as the optimal concentration.

**Calibration Curve for Glucose Determination.** Different concentrations of glucose were added to the homogeneous solution containing HRP, TMB, GOx and HCl under the optimized conditions. A gradual blue-shift of LSPR was observed in Fig. 5A. As presented in Fig. 5B, the longitudinal LSPR shift had a linear correlation with the concentration of glucose in the range between 0.1 and 0.9 mM. Furthermore, different colors appeared with different concentrations of glucose (Fig. 5C). Accordingly, the concentration of glucose can be well determined via vivid color change with high sensitivity, which can be observed by naked eyes at a glance. Interference studies were done to explore the specific detection of glucose in human serum using this sensor, including investigation of most commonly existing substances in human serum such as fructose, sucrose, ascorbic acid (AA), uric acid (UA) and a series of amino acids (glutamic acid, glycine, histidine, alanine, tyrosine, serine, and phenylalanine). Given the approximate amount of these samples in serum and quantity demand of real samples, different concentrations of abovementioned interferences were separately added to the detection system with 0.5 mM of glucose. The absorbance results barely changed, indicating these interferences hardly affect the glucose sensing (Fig. 6A). Furthermore, Fig. 6B also demonstrated the excellent sensitivity of the assay using the same interferences. This is

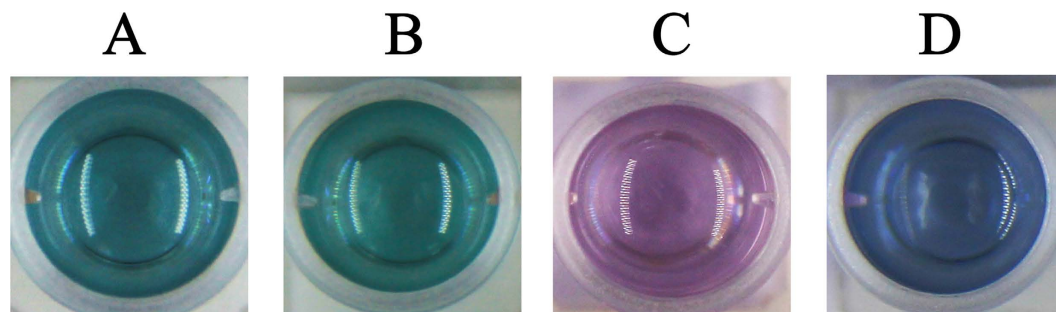


**Figure 7.** The solution color of AuNRs for the corresponding human serum samples in Table 1.

Sample	Glucose (mM)	
	Calculated value	This method
A	4.8	4.0~5.0
B	4.5	4.0~5.0
C	7.2	7.0~8.0
D	5.7	5.0~6.0

**Table 1.** Visual detection for glucose in human serum.

probably due to the specificity between GOx and glucose. Thus this result demonstrates that the proposed multi-color glucose sensor owns superior selectivity.

**Visual Detection of Glucose in Serum Samples.** Serum samples obtained from the volunteers were firstly diluted 10 times. The results reveal that the solution colors present green, blue and purple (Fig. 7). According to the above standard colorimetric figure, the concentration of glucose in Sample A was inferred to be between 4.0 and 5.0 mM, which was close to the calculated value of 4.8 mM, and the Sample B to D obeyed the same rule (Table 1). When the solution color turn to purple, it means the blood-sugar level is out of normal value (approximately 7.0 mM). These results indicate that our proposed multicolor glucose sensor has great potential application in the detection of real samples.

## Conclusions

In conclusion, a multicolor glucose sensor has been proposed due to the special optical property of AuNRs and the etching of AuNRs by TMB<sup>2+</sup>. As the glucose concentration increased, the LSPR band of AuNRs had a blue-shift and the solution showed the vivid colors from the reddish brown, gray, green, blue, purple, pink to yellow. The visual detection for glucose is achieved by naked eyes with the advantages of speediness, simplicity, and low cost.

## References

- Saha, K., Agasti, S. S., Kim, C., Li, X. & Rotello, V. M. Gold nanoparticles in chemical and biological sensing. *Chemical reviews* **112**, 2739–2779, doi: 10.1021/cr2001178 (2012).
- Zhang, J. *et al.* Quantifying the dissolution of nanomaterials at the nano-bio interface. *Science China Chemistry* **58**, 761–767 (2015).
- Xianyu, Y. *et al.* An ultrasensitive, non-enzymatic glucose assay via gold nanorod-assisted generation of silver nanoparticles. *Nanoscale* **5**, 6303–6306, doi: 10.1039/c3nr01697h (2013).
- Guo, L., Xu, Y., Ferhan, A. R., Chen, G. & Kim, D. H. Oriented gold nanoparticle aggregation for colorimetric sensors with surprisingly high analytical figures of merit. *J Am Chem Soc* **135**, 12338–12345, doi: 10.1021/ja405371g (2013).
- Coronado-Puchau, M., Saa, L., Grzelczak, M., Pavlov, V. & Liz-Marzán, L. M. Enzymatic modulation of gold nanorod growth and application to nerve gas detection. *Nano Today* **8**, 461–468, doi: 10.1016/j.nantod.2013.08.008 (2013).
- Kou X. *et al.* Glutathione- and cysteine-induced transverse overgrowth on gold nanorods. *J Am Chem Soc* **129**, 6402–6404, doi: 10.1021/ja0710508 (2007).
- Tsung, C. K. *et al.* Selective shortening of single-crystalline gold nanorods by mild oxidation. *J Am Chem Soc*, **128**, 5352–5353, doi: 10.1021/ja060447t (2006).
- Guo X. *et al.* Lateral etching of core-shell Au@ metal nanorods to metal-tipped Au nanorods with improved catalytic activity. *ACS nano* **6**, 1165–1175, doi: 10.1021/nn203793k (2012).
- Ni, W. *et al.* Tailoring longitudinal surface plasmon wavelengths, scattering and absorption cross sections of gold nanorods. *ACS Nano* **2**, 677–686, doi: 10.1021/nn7003603 (2008).
- Chandrasekar, G., Mougín, K., Haidara, H., Vidal, L. & Gnecco, E. Shape and size transformation of gold nanorods (GNRs) via oxidation process: A reverse growth mechanism. *Appl. Surf. Sci* **257**, 4175–4179, doi: 10.1016/j.apsusc.2010.12.015 (2011).
- Lou, T. *et al.* Colorimetric detection of trace copper ions based on catalytic leaching of silver-coated gold nanoparticles. *ACS Appl Mater Interfaces* **3**, 4215–4220, doi: 10.1021/am2008486 (2011).
- Liu, R. *et al.* Colorimetric sensing of copper(II) based on catalytic etching of gold nanoparticles. *Talanta* **112**, 37–42, doi: 10.1016/j.talanta.2013.01.065 (2013).
- Zou, R. *et al.* Selective etching of gold nanorods by ferric chloride at room temperature. *Cryst Eng Comm* **11**, 2797, doi: 10.1039/b911902g (2009).

14. Shang, L., Jin, L. & Dong, S. Sensitive turn-on fluorescent detection of cyanide based on the dissolution of fluorophore functionalized gold nanoparticles. *Chem Commun (Camb)* 3077–3079, doi: 10.1039/b902216c (2009).
15. Tripathy, S. K., Woo, J. Y. & Han, C. S. Highly selective colorimetric detection of hydrochloric acid using unlabeled gold nanoparticles and an oxidizing agent. *Anal Chem* **83**, 9206–9212, doi: 10.1021/ac202500m (2011).
16. Liu, J.-M. *et al.* A promising non-aggregation colorimetric sensor of AuNRs–Ag<sup>+</sup> for determination of dopamine. *Sens. Actuators B* **176**, 97–102, doi: 10.1016/j.snb.2012.08.083 (2013).
17. Wu, G. W. *et al.* Citrate-capped platinum nanoparticle as a smart probe for ultrasensitive mercury sensing. *Anal Chem* **86**, 10955–10960, doi: 10.1021/ac503544w (2014).
18. Chen, Z. *et al.* Colorimetric sensing of copper(ii) based on catalytic etching of gold nanorods. *RSC Advances* **3**, 13318, doi: 10.1039/c3ra40559a (2013).
19. Zhang, Z., Chen, Z., Qu, C. & Chen, L. Highly sensitive visual detection of copper ions based on the shape-dependent LSPR spectroscopy of gold nanorods. *Langmuir* **30**, 3625–3630, doi: 10.1021/la500106a (2014).
20. Saa, L., Coronado-Puchau, M., Pavlov, V. & Liz-Marzan, L. M. Enzymatic etching of gold nanorods by horseradish peroxidase and application to blood glucose detection. *Nanoscale* **6**, 7405–7409, doi: 10.1039/c4nr01323a (2014).
21. Liu, X. *et al.* A plasmonic blood glucose monitor based on enzymatic etching of gold nanorods. *Chem Commun (Camb)* **49**, 1856–1858, doi: 10.1039/c3cc38476d (2013).
22. Ma, X. *et al.* A universal multicolor immunosensor for semiquantitative visual detection of biomarkers with the naked eyes. *Biosens. Bioelectron* **87**, 122–128, doi: 10.1016/j.bios.2016.08.021 (2016).
23. Josephy, P. D., Eling, T. & Mason, R. P. The horseradish peroxidase-catalyzed oxidation of 3,5,3',5'-tetramethylbenzidine. Free radical and charge-transfer complex intermediates. *J. Biol. Chem* **257**, 3669–3675 (1982).
24. Jiao, K. A thin-layer spectroelectrochemical study of 3,3',5,5'-tetramethylbenzidine at SnO<sub>2</sub>: F film optically transparent electrode. *Sci. China, Ser. B: Chem* **47**, 267, doi: 10.1360/03yb0174 (2004).

## Acknowledgements

This project was financially supported by the Natural Science Foundation of China (21575027, 21675028, 21375021, 21275031, and 21277025), the Natural Science Foundation of Fujian Province for Distinguished Young Scholar (2014J06005) and the Program for Changjiang Scholars and Innovative Research Team in University (No. IRT1116).

## Author Contributions

Z.-Y.L., X.-M.M. and L.-H.G. designed the research; Y.L., M.-M.Z., Y.-J.G., F.L. and X.-M.M. performed the experiments; B.Q., Z.-Y.L., and G.-N.C. contributed to the reagents/materials/analysis tools; Y.L., Z.-Y.L. and L.-H.G. wrote the paper; all authors approved the final manuscript.

## Additional Information

**Competing financial interests:** The authors declare no competing financial interests.

**How to cite this article:** Lin, Y. *et al.* Multicolor Colorimetric Biosensor for the Determination of Glucose based on the Etching of Gold Nanorods. *Sci. Rep.* **6**, 37879; doi: 10.1038/srep37879 (2016).

**Publisher's note:** Springer Nature remains neutral with regard to jurisdictional claims in published maps and institutional affiliations.



This work is licensed under a Creative Commons Attribution 4.0 International License. The images or other third party material in this article are included in the article's Creative Commons license, unless indicated otherwise in the credit line; if the material is not included under the Creative Commons license, users will need to obtain permission from the license holder to reproduce the material. To view a copy of this license, visit <http://creativecommons.org/licenses/by/4.0/>

© The Author(s) 2016